INSTITUTE OF PHYSICS PUBLISHING PLASMA PHYSICS AND CONTROLLED FUSION

Plasma Phys. Control. Fusion **45** (2003) 1–23 PII: S0741-3335(03)52168-6

ICPP-CLUSTER

Turbulent transport reduction by $E \times B$ velocity shear during edge plasma biasing: recent experimental results

G Van Oost[1], J Adámek[2], V Antoni[3], P Balan[4], J A Boedo[5], P Devynck[6], I Ďuran[2], L Eliseev[7], J P Gunn[6], M Hron[2], C Ionita[4], S Jachmich[8], G S Kirnev[7], E Martines[3], A Melnikov[7], R Schrittwieser[4], C Silva[9], J Stöckel[2], M Tendler[10], C Varandas[9], M Van Schoor[8], V Vershkov[7] and R R Weynants[8]

[1] Department of Applied Physics, Ghent University, Ghent, Belgium
[2] Institute of Plasma Physics, Association EURATOM/IPP.CR, Prague, Czech Republic
[3] Consorzio RFX, Associazione EURATOM-ENEA sulla Fusione, Padova, Italy
[4] Department of Ion Physics, University of Innsbruck, Innsbruck, Austria
[5] Department of Mechanical and Aerospace Engineering, University of California, San Diego, La Jolla, CA, USA
[6] Association EURATOM/CEA sur la fusion contrôlée, Saint Paul Lez Durance, France
[7] RRC Kurchatov Institute, Moscow, Russian Federation
[8] Laboratoire de Physique des Plasmas–Laboratorium voor Plasmafysica, Association 'Euratom-Belgian state', Ecole Royale Militaire—Koninklijke Militaire School, B-1000 Brussels, Belgium (Partner in the Trilateral Euregio Cluster)
[9] Centro de Fusão Nuclear—Association EURATOM/IST, Instituto Superior Técnico, Lisboa, Portugal
[10] Alfvén Laboratory, Royal Institute of Technology, Stockholm, Sweden

E-mail: g.vanoost@fz-juelich.de

Received 9 August 2002
Published
Online at stacks.iop.org/PPCF/45

Abstract

Experiments in the tokamaks TEXTOR, CASTOR, T-10 and ISTTOK, as well as in the reversed field pinch RFX have provided new and complementary evidence on the physics of the universal mechanism of $E \times B$ velocity shear stabilization of turbulence, concomitant transport barrier formation and radial conductivity by using various edge biasing techniques.

In TEXTOR the causality between transport reduction and induced electric fields in the edge has been for the first time clearly demonstrated. The high electric field gradients have been identified as the cause for the quenching of turbulent cells. A quantitative analysis of the measured transport reduction is in good agreement with theoretical predictions. The scaling of plasma turbulence suppression with velocity shear has been established, revealing the density-potential cross-phase as a key element. Reduction in poloidal electric field, temperature, and density fluctuations across the shear layer lead to a reduction

of the anomalous conducted and convected heat fluxes resulting in an energy transport barrier that is measured directly.

In CASTOR the biasing electrode is placed at the separatrix in a non-intrusive configuration which has demonstrated strongly sheared electric fields and consequent improvement of the global particle confinement, as predicted by theory. The impact of sheared $E \times B$ flow on edge turbulent structures has been measured directly using a comprehensive set of electrostatic probe arrays as well as emissive probes. Measurements with a full poloidal Langmuir probe array have revealed quasi-coherent electrostatic waves in the SOL with a dominant mode number equal to the edge safety factor.

In T-10 edge biasing is clearly improving the global performance of ECR heated discharges. Reflectometry and heavy ion beam probe measurements show the existence of a narrow plasma layer with strong suppression of turbulence.

On ISTTOK, the influence of alternating positive and negative electrode and (non-intrusive) limiter biasing has been compared. Electrode biasing is found to be more efficient in modifying the radial electric field E_r and confinement, limiter biasing acting mainly on the SOL.

In the RFX reversed field pinch it has been demonstrated that also in RFPs biasing can increase the local $E \times B$ velocity shear in the edge region, and hence substantially reduce the local turbulence driven particle flux mainly due to a change in the relative phase between potential and density fluctuations.

1. Introduction

The understanding and reduction of turbulent transport in magnetic confinement devices is not only an academic task, but also a matter of practical interest, since high confinement is chosen as the regime for ITER and possible future reactors since it reduces size and cost.

An extensive review on the physical mechanisms determining the radial electric field in a toroidal plasma has been published by Ida [1]. He describes amongst others the effect of variations in the radial electric field and shear in the bulk rotation velocity on the improvement of transport properties. Since the pioneering work on the tokamak CCT [2], many papers have been devoted to the effect of electric field biasing in specific machines (see, e.g. reviews [3–5]), which in general leads to a strongly varying radial electric field as a function of radius and a resulting sheared $E \times B$ flow, giving rise to improved confinement properties. Due to space limitation, a historical overview of edge biasing work will not be given here, and the collection of material is limited. This paper attempts at bridging the gap between the early and the new, more detailed understanding.

The importance of radial electric fields for plasma transport was in the past repeatedly established. Since the discovery of the transition from a low confinement mode (L-mode) to a high confinement mode (H-mode) in 1982 [6], a flurry of activity started with the experimental and theoretical recognition of a link between E_r and the formation of edge and internal transport barriers in toroidal plasmas. The importance of radial electric field shear in the L–H transition was suggested for the first time in [7, 8]. The (spontaneous) H-mode has been obtained in a variety of tokamaks mainly with elongated plasma cross-section and divertor, and recently also in the limiter tokamak T-10 with ECRH as the only auxiliary heating. An (induced) H-mode can also be triggered externally by imposing an electric field and the resulting $E \times B$

rotation in tokamaks like TEXTOR, CASTOR, T-10 and ISSTOK, as well as in reversed field pinches like RFX. These electrode biasing (EB) experiments have contributed significantly to the understanding of the H-mode phenomenon and of the effects of E_r on plasma transport.

The L–H transition is accompanied by a reduction of turbulent transport, confirming the paradigm that microturbulence is responsible for a considerable part of energy and particle losses. The shearing of turbulent eddies by differential $E \times B$ flow velocity has been proposed as a universal mechanism to stabilize turbulence in plasmas [9], a hypothesis supported by early work on the tokamak TEXT [10], and has been observed with different magnetic configurations. The $E \times B$ velocity shear can suppress turbulence due to linear stabilization of turbulent modes, and in particular non-linearly by decorrelation of turbulent vortices, thereby reducing transport by acting on both the amplitude of the fluctuations and the phase between them [11]. The shearing rate, $\omega_{E\times B}$, must be comparable to $\Delta\omega_D$, the non-linear turbulence decorrelation rate in the absence of shear.

This paper reports on recent results of a coordinated study of radial electric fields (E_r) and their role in the establishment of edge transport barriers and improved confinement in the circular limiter tokamaks TEXTOR in Jülich, CASTOR in Prague, and T-10 in Moscow, where E_r is externally applied to the plasma in a controlled way using a biased electrode. Edge biasing is the controlled creation of radial electric fields by driving a current through the edge plasma inside the last closed flux surface (LCFS). In the circular limiter tokamak ISSTOK in Lisbon E_r is externally applied by DC or AC electrode or limiter biasing (LB). In the reversed field pinch RFX in Padova electrodes are inserted into the plasma edge to modify the $E \times B$ velocity and its shear.

Since the early 1990s pioneering research has been conducted on TEXTOR ($R = 1.75$ m, $a = 0.46$ m) in the domain of edge radial electric fields using EB. The physics of radial currents was studied and the radial conductivity in the edge of TEXTOR was found to be dominated by recycling (ion-neutral collisions) at the LCFS and by parallel viscosity inside the LCFS. The destruction of parallel viscosity by strong poloidal plasma rotation was verified and found to lead to bifurcation in the electric field. The mechanism of reduction of electrostatic turbulence due to a shear in the $E \times B$ flow, and the causality between the two were demonstrated. Particle and energy confinement improve as a particle as well as heat transport barrier are established in the plasma edge. An H-mode-like behaviour can be induced both with positive and negative electric fields, although negative biasing is limited by the ion saturation current of the electrode.

The impact of sheared radial electric fields on turbulent structures and flows at the plasma edge is investigated on the CASTOR tokamak ($R = 0.4$ m, $a = 0.085$ m). A non-intrusive biasing scheme called 'separatrix biasing' whereby the electrode is located in the scrape-off layer (SOL) with its tip just touching the LCFS was found to be efficient, as predicted by theory [12]. There is evidence of a strongly sheared radial electric field and $E \times B$ flow, resulting in the formation of a transport barrier at the separatrix. Advanced probe diagnosis of the edge region has shown that the $E \times B$ shear rate that arises during separatrix biasing is larger than for standard edge plasma biasing (with the electrode inserted inside the LCFS as in TEXTOR). The plasma flows, especially the poloidal $E \times B$ drift velocity, are strongly modified in the sheared region, reaching Mach numbers as high as half the sound speed. The corresponding shear rates ($\sim 5 \times 10^6\ \mathrm{s}^{-1}$) derived from both the flow and electric field profiles are in excellent agreement and are at least an order of magnitude higher than the growth rate of unstable turbulent modes as estimated from fluctuation measurements. The poloidal symmetry of SOL turbulence has been investigated using a full poloidal array of Langmuir probes.

During EB combined with ECRH (at power levels below the threshold for spontaneous L–H transition) in the tokamak T-10 ($R = 1.5$ m, $a = 0.3$ m), a regime of improved confinement is obtained with features resembling those of the H-mode in other tokamaks.

This H-mode with ECRH as the only auxiliary heating method is studied using a heavy ion beam probe (HIBP) which allows to investigate directly the plasma potential in the core and edge plasma, and simultaneously the electron density profile. Reflectometer and HIBP measurements have shown a reduction of turbulence in the shear layer.

On the ISTTOK tokamak ($R = 0.46$ m; $a = 0.085$ m), the influence of alternating positive and negative EB and LB is studied. EB is found to be more efficient in modifying E_r and confinement. The best confinement improvement is obtained with positive EB, showing a good correlation between confinement changes and $E \times B$ shear. Negative (positive) LB leads to improved (deteriorated) confinement and better (worse) stability of the plasma column.

In the RFX reversed field pinch experiment ($R = 2$ m; $a = 0.457$ m) two biasing electrodes have been inserted well inside the LCFS. It has been demonstrated that also in RFPs biasing can increase the local $E \times B$ velocity shear in the edge region, and hence substantially reduce the local turbulence driven particle flux mainly due to a change in the relative phase between potential and density fluctuations.

2. Scaling of turbulence with shear, and causality between $E \times B$ shear and transport barrier formation (TEXTOR)

2.1. Experimental set-up

The set-up of the edge polarization experiment is shown in figure 1. The electrode has a mushroom-shaped head that is inserted about 5 cm beyond the toroidal belt limiter (ALT-II). The voltage is applied between the electrode and the limiter, which is grounded to the potential of the first plasma-facing wall (named as liner). An insulating boron-nitride sleeve assures that the bias potential is only imposed on flux surfaces intersecting the electrode head. More details on EB in TEXTOR can be found in [13, 14].

Usually the bias voltage V_{E} in the experiments reported here was varied over time from 0 up to maximum 600 V. The plasma parameters are $B_{\mathrm{t}} = 2{:}33$ T, $I_{\mathrm{P}} = 210$ kA and the pre-bias central line-averaged electron density $n_{\mathrm{e}} = 1 \times 10^{19}\,\mathrm{m}^{-3}$. The spatial location and the magnitude of the electric field are imposed by the magnitude of the radial current and by the profile of the radial conductivity σ_r, determined by parallel viscosity and ion–neutral collisions [15]. The radial electric field follows the increasing voltage until bifurcation occurs, where E_r suddenly jumps to higher values. At the same time the electrode current I_{E} drops, causing the power supply to oscillate, imposing rapid changes of the radial current density j_r. This rapid oscillation has been used as a convenient tool to investigate causality.

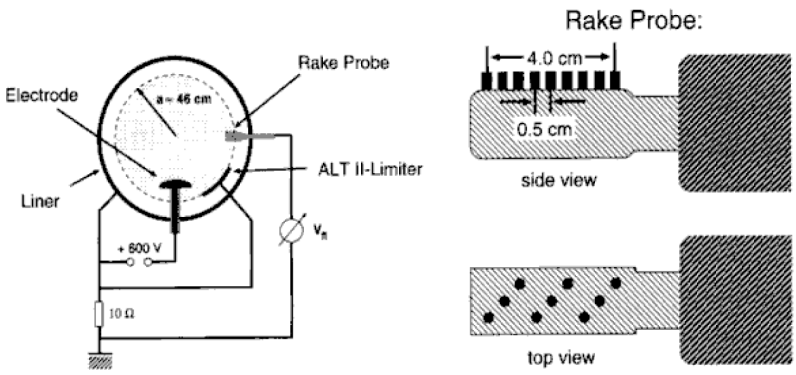

Figure 1. Schematic drawing of the polarization set-up and of the rake probe.

The radial electric fields are determined using a Langmuir probe (rake probe) consisting of a boron-nitride head carrying 16 carbon (CFC) tips (length 4 mm, radius 1.6 mm), radially distributed over 4 cm, and measuring the profile of the floating potential $V_{\rm fl}$ with a radial resolution of 3.5 mm. The tips are aligned perpendicularly to the magnetic field such that probe shadowing is avoided. The probe is at a fixed position during the whole discharge. The radial electric field is then found as

$$E_r = -\nabla V_{\rm pp} \approx -\nabla V_{\rm fl} - \frac{3k\nabla T_{\rm e}}{e},$$

where $V_{\rm pp}$ is the plasma potential. Since in these experiments $\nabla V_{\rm fl}$ is of order 100 V cm^{-1}, we neglect the contribution from the temperature gradient, which is typically less than 10 eV cm^{-1} and remains small in the high confinement regime. The time resolution of the rake probe is 40 μs.

Mach probes were tested and optimized to determine parallel and perpendicular particle flows in the plasma edge and SOL [16], allowing together with the well diagnosed pumped toroidal belt limiter ALT-II the study of particle exhaust.

The electron density profiles are obtained by means of Langmuir probes as well of a Li-beam spectroscopy diagnostic. As a key issue in this investigation is the detailed spatial and temporal correlation of the field and density changes, it is important to note that the atomic beam and the rake probe are mounted at the same equatorial outboard port, toroidally separated only by 12 cm, which minimizes errors in determining their relative radial allocation.

Changes in the global particle confinement time $\tau_{\rm p}$ are inferred from the ratio of the total number of electrons in the discharge $N_{\rm e}^{\rm tot}$ to the total ionization rate at the plasma periphery (i.e. the hydrogen source term). The latter requires a detailed book-keeping of recycling at the limiter, the wall and the electrode.

Turbulence data were obtained with a fast reciprocating probe array featuring five 1.5 mm $\times$ 1.5 mm tips for simultaneous measurements of fluctuating floating potentials, poloidal and radial electric fields and local plasma density. The data were digitized at 10 bit and 1 MHz. The power spectra of the density, potential and temperature fluctuations are significant only up to 200 kHz. The temperature fluctuations are measured using the harmonics technique [17].

2.2. Experimental results

2.2.1. Causality. EB experiments are a standard scenario on TEXTOR to study the H-mode. The electrode voltage $V_{\rm E}$ is slowly ramped up to 600 V during the flat top phase of the discharge. The radial electric field follows the increasing voltage until a bifurcation occurs, where the electric field suddenly jumps to higher values. At the same time the electrode currents $I_{\rm E}$ drops, causing the power supply to oscillate (see figure 2(a), red lines), and imposes rapid changes of the radial current j_r. This rapid oscillation will be used in this paper as a convenient tool to establish causality. The electric field, generated by j_r, not only sets-up a poloidal rotation, but also reduces the parallel viscosity, leading to a non-linearity in the radial conductivity. At a certain value of the electric field the viscosity is destroyed, the plasma spins-up and the bifurcation is triggered. Although at this time very high electric fields and shear rates are achieved, we like to point out that the transport and the confinement, represented by total number of confined electrons $N_{\rm e,tot}$ and edge recycling H_α in figure 2(b) [18], are affected already prior to bifurcation.

The magnitude and location of the electric field gradient ∇E_r depend on the radial conductivity profile σ_r. As the electrode voltage $V_{\rm E}$ is increased, ∇E_r changes at the rate of the local σ_r until E_r is high enough to squeeze the banana orbits of the particles and to

destroy the parallel viscosity ('bifurcation'). This triggered and drastic decrease of σ_r causes ∇E_r to jump to much higher values. Since V_E is afterwards still increased, ∇E_r grows further, but at a smaller rate. Since the timescale of the orbit squeezing effect is very short no hysteresis between ∇E_r and V_E is visible during the voltage oscillations. The edge transport, monitored by ∇n_e and H_α, and the core confinement, react to the oscillating voltage and the imposed ∇E_r changes, as shown by the time traces in figure 2(b). During the oscillating phase, ∇E_r changes on a timescale of 1 ms, which is shorter than the typical particle confinement time. Since the turbulence needs to adjust, the effect on the particle transport and confinement is delayed and a hysteresis between the particle diffusion coefficient D and ∇E_r develops. As seen in figure 3 the electric field gradient is leading the formation of the transport barrier,

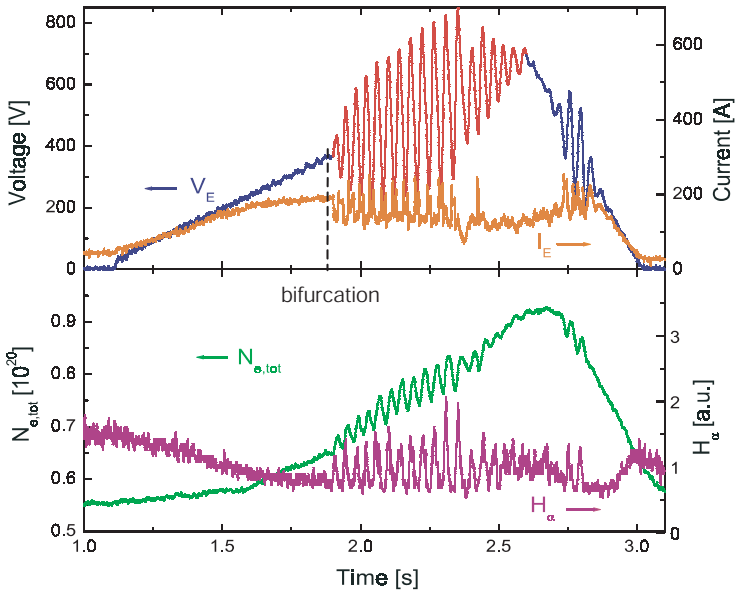

Figure 2. Time traces of electrode voltage V_E and current I_E, total number of confined electrons $N_\mathrm{e,tot}$ and edge recycling H_α.

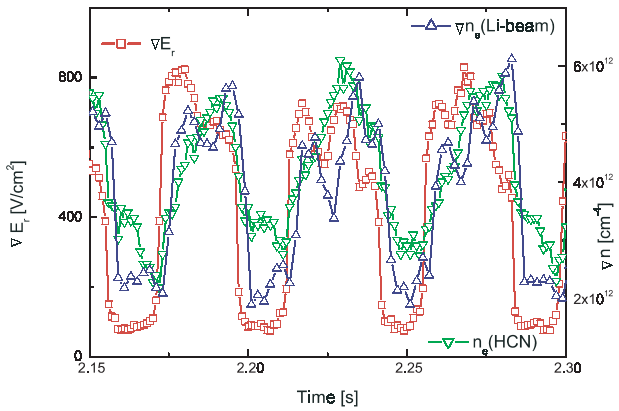

Figure 3. ∇E_r is leading changes in ∇n_e and n_e (HCN). The density gradient is measured at the same location as the electric field gradient.

represented by the density gradient at the same location, by about 5 ms. The time resolution of the electric field measurements is 40 μs and that of the edge density 2 ms. To corroborate our findings, the outermost interferometer channel, which has a time resolution of 200 μs, is displayed in figure 3. The delay in the density is $\approx$5.6 ms. Also note that the particle transport exhibits similar fine structures in time as ∇E_r does, which illustrates the firm link between D and ∇E_r.

In spite of the fact that the radial electric field is imposed by biasing, the observed causality between ∇E_r and ∇n_e is not trivial, as one could think considering the ion radial force balance equation. In our experiment, the voltage difference is applied between the electrode and the limiter, distant by some 5 cm. However, the electric field is not just the voltage difference divided by the distance, but is confined over a much narrower region, on account of the radial conductivity profile. Be it therefore through an intricate mechanism, it is nevertheless obviously the biasing that causes this field to develop, but this field in itself is not the cause of the density steepening. The radial force balance equation asks for a steeper density gradient as a result of a stronger negative electric field or vice versa. In our case the density gradient steepens when the field grows more positive (the reason that this is possible being the observed very strong poloidal rotation).

2.2.2. Scaling of turbulence with shear. First quantitative studies of the effects of $E \times B$ flow shear on turbulence have been carried out on TEXTOR [19–21]. In [20] the critical $E \times B$ flow shear has been introduced, which corresponds to the electrical field gradient for which the poloidal turbulence shearing rate τ_s^{-1} is equal to the turbulence decorrelation rate τ_{co}^{-1}. Assuming the turbulence to be isotropic we find for the critical electric field gradient

$$\nabla E_{crit} = \sqrt{2}(k_\perp^2 D)_0 B_t(r). \tag{1}$$

The critical field gradient is a measure for how efficient an induced $E \times B$ flow shear can quench turbulent transport. Higher values for ∇E_{crit} indicate that more shear has to be applied in order to achieve the same amount of turbulence suppression.

Even for infinite shear a certain level of transport will remain, which will be denoted by D_{rest}, whereas the part of the particle transport subject to be quenched by the $E \times B$ shear is considered to be the anomalous diffusion D_{ano}. In [22] a generic form for the change of the particle diffusion coefficient D independent of the specific poloidal shear mechanism has been proposed, which can be written with the help of the definition of equation (1) as

$$D = D_{rest} + \frac{D_{ano}}{1 + (\nabla E_r / \nabla E_{crit})^\gamma}. \tag{2}$$

The exact value of the exponent γ depends on the model assumed for the non-linear decorrelation. In case of strong shear Biglari *et al* [9] proposed $\gamma = \frac{2}{3}$. If only weak shear is present, Shaing *et al* [23] found $\gamma = 2$. Zhang and Mahajan (ZM) [24] have concluded $\gamma = 2$ for arbitrary shear. Our analysis shows γ to be in the range of 2–4.

The exponent γ was found for the fit of the diffusion coefficient to be 2.9 and for the particle confinement time to be 2.3. The non-uniform decrease of κ_D in the vicinity of ∇E_{crit} could point to a multi-mode feature of the turbulence.

The first extensive characterization of turbulence with electric biasing was made in TEXTOR [25]. Reciprocating probe data on the scaling of the normalized turbulent density and particle flux and to the density-potential cross-phase were collected [26]. Fits to the data were made based on existing theories and also with similar functional forms but and exponential free parameter to explore deviation from predictions. As shown in figure 4 the normalized density fluctuations scaling is well fitted by the ZM [24] prediction (exponent 2) although

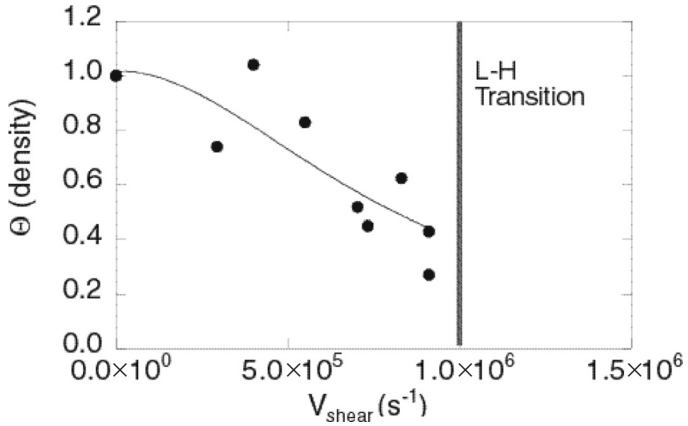

Figure 4. Scaling of normalized density fluctuations with shear (●) and the fit by the ZM prediction (——). The shear at which the L–H transition occurs is marked.

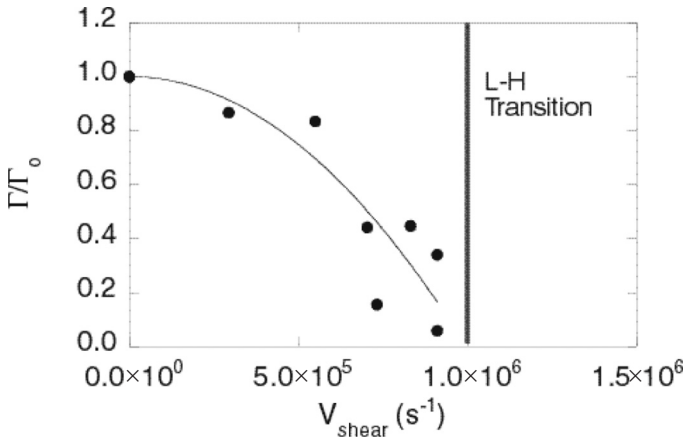

Figure 5. Scaling of normalized radial particle flux with shear (●) and the fit (——) based on Ware–Terry predictions.

similar quality fits can be obtained with an exponent of 3.6. No difference is found between positive and negative shear.

As shown in figure 5 the radial flux scaling was fitted by a function *à la* Ware–Terry [11] satisfactorily (exponent 2) and it is found that the same function with free-parameter exponent converges at a value of 1.67 with similar quality fit. Finally the cross-phase term is found to show measurable sensitivity to the sign of the shear and most importantly, to become negative in H-mode conditions. Two important results should be noted: first, that the scaling of the cross-phase term is as strong as that of the turbulence amplitudes, revealing the cross-phase as a key element in the suppression of turbulent transport (see also the RFX results, section 6). Second, that there is a difference in the scaling of the cross-phase between the positive and negative shear regions, an effect not included in the theories, which are phase-sign blind and therefore these results should be considered closely by theoreticians.

In general, theories proposing a scaling that makes the amplitudes drop roughly as $|\mathrm{d}v_{\mathrm{E}}/\mathrm{d}r|^2$ seem to reproduce the amplitude and flux data but a somewhat stronger dependence (2.6) may be needed for the cross-phase term.

For the first time the suppression of T_e fluctuations in a strongly sheared velocity field have been measured, as predicted by theory if parallel thermal conduction is not dominant [27]. Reductions in poloidal electric field, temperature and density fluctuations across the shear layer lead to a reduction of the anomalous conducted and convected heat fluxes resulting in an energy transport barrier that is measured directly. Anomalous conduction is ∼10 times greater than anomalous convection in OH conditions and the latter shows a dependence on higher derivatives of the shear velocity.

3. $E \times B$ flow measurements and structure of edge turbulence (CASTOR)

3.1. Set-up of biasing experiments

CASTOR is a small tokamak with circular cross-section, major radius $R = 0.4$ m. The minor radius is defined by a poloidal limiter with $a = 60$ or 85 mm. The experiments are performed in a hydrogen plasma at a toroidal magnetic field $B_t = 1$ T, plasma current $I_p = 6$–15 kA and line average density $n_e = 1$–2×10^{19} m^{-3}. In the SOL region, the plasma density varies in the range 0.2–1 $\times 10^{18}$ m^{-3} and the electron temperature is 8–25 eV.

The impact of sheared electric fields on the structure of edge fluctuations and plasma flows is investigated on the CASTOR tokamak with a non-intrusive biasing scheme, whereby a mushroom-like electrode (made of carbon) is located in the SOL, but its top is just touching the separatrix (see figure 6).

In such a scheme, called 'separatrix biasing', the potential is affected only in a relatively narrow region near the separatrix and the radial electric field is amplified at both sides of the electrode, because, in contrast to the standard biasing arrangement, the bulk plasma remains unbiased. Consequently, the radial electric field is highly sheared in the separatrix region and affects there significantly the plasma flows and the turbulent structures. This situation, shown schematically in the right panel of figure 6, has been confirmed experimentally by measuring the radial profile of the plasma potential inside the plasma column [28]. Since the biased electrode is hidden in the SOL, the thermal load should certainly be smaller than

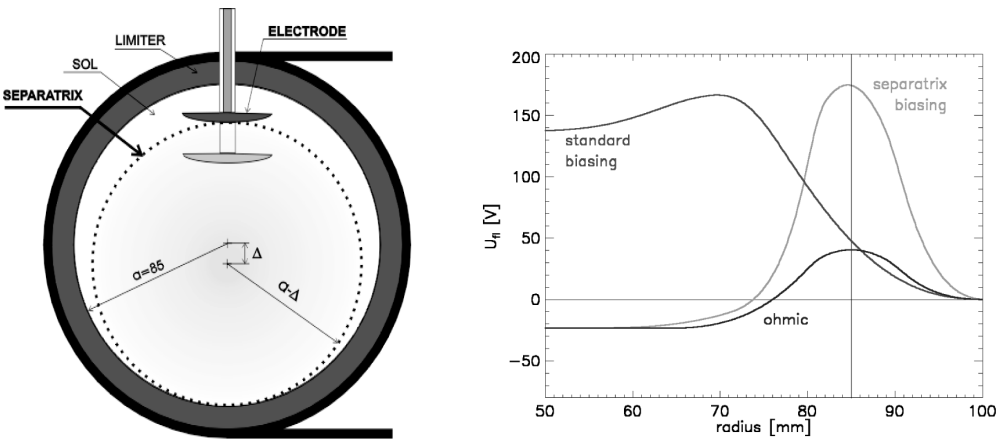

Figure 6. Left: poloidal cross-section of the CASTOR tokamak, schematically showing the respective position of plasma column and biasing electrode at the 'standard' and at the 'separatrix biasing' arrangements. Right: comparison of radial profiles of floating potential in Ohmic and biasing cases (schematically). Here, the separatrix is at 85 mm. Position of the electrode at standard biasing scheme is 70 mm.

in the standard configuration. This offers practical applications of this scheme in large-scale experiments.

This experiment has been predicted theoretically [12]; in order to trigger an L–H transition, the model requires a value of the electric field larger than that given by neoclassical theory. At the separatrix the electric field within the SOL is governed by a contact with plates. This has to match the self-generated electric field on closed field lines governed by plasma flows and magnetic field geometry. Therefore, the peripheral plasma plays the crucial role in controlling the global confinement and affecting plasma profiles and local transport diffusivities [29]. When a current of about 35–40 A is drawn by the electrode during the biasing period, the global particle confinement improves in both cases (by 80% for the 'standard' configuration and by about 50% at separatrix biasing). However, the H_α emission slightly increases during separatrix biasing, which indicates a slight enhancement of recycling.

3.2. Fluctuation and flow measurements

In the CASTOR tokamak, which is probably the world-leading machine for probe research, a plenitude of electric and magnetic probes has been used to study the edge plasma and its fluctuations. The edge turbulence was analysed by a poloidal array of 16 Langmuir tips to deduce the characteristic dimension and lifetime of density and potential fluctuations and their propagation velocity and mutual correlation (the fluctuation induced flux) [30]. The main result of these studies is that the edge turbulence in the CASTOR tokamak is generally the same (or similar) as in larger experiments with toroidal geometry such as ASDEX tokamak and W7-AS stellarator [31]. The rake probe (16 tips) is routinely used to measure the radial profiles at the plasma edge during a single shot. Such an array was found to be useful to determine the instantaneous radial profile of the floating potential, from which the radial electric field and its gradient can be determined [32]. The two-dimensional matrix (8×6) of Langmuir tips has been used to study properties of the edge turbulence simultaneously in the radial and poloidal direction; long living, quasi-coherent structures of potential have been identified in the SOL [33, 34]. The main ion flow velocity is measured by a rotatable Mach probe, which allows to determine the parallel and perpendicular velocities with the temporal resolution $\sim$3 ms and to check existing models [16, 35, 36]. Very recently, a novel concept has been suggested to measure the electron temperature fluctuations [37] and a prototype of the so-called tunnel probe has been successfully tested on CASTOR [38]. Several examples of probe measurements are discussed below.

3.2.1. Optimized (ideal) Gundestrup probe (IGP). The optimized Gundestrup probe [39] was used to compare ion flows with the phase velocity of fluctuations moving poloidally across the Gundestrup collectors. The ion mass flow is measured by the standard arrangement, i.e. signals of all the segments are digitized at a standard sampling rate. From these data, the perpendicular Mach number of the ion flow is derived. Simultaneously, the signals from the most upstream and downstream pairs of the segments are recorded faster, at a sampling rate of $5\,\mathrm{MS\,s^{-1}}$. Then, the cross-correlation function is calculated and the transit time of a poloidally localized structure across the corresponding segments is deduced from the shift of its maximum. In figure 7 we compare four measurements of the poloidal velocity deduced from (1) the IGP polar diagrams, (2) the phase velocity of structures moving across the upstream segments, (3) the phase velocity of structures moving across the downstream segments, and (4) the $E \times B$ drift speed calculated from the radial electric field using the rake probe.

In both the Ohmic and biased phases of the discharge, all methods give the same sign of the velocity and roughly the same inversion radius. From figure 7 it is evident that the $E \times B$

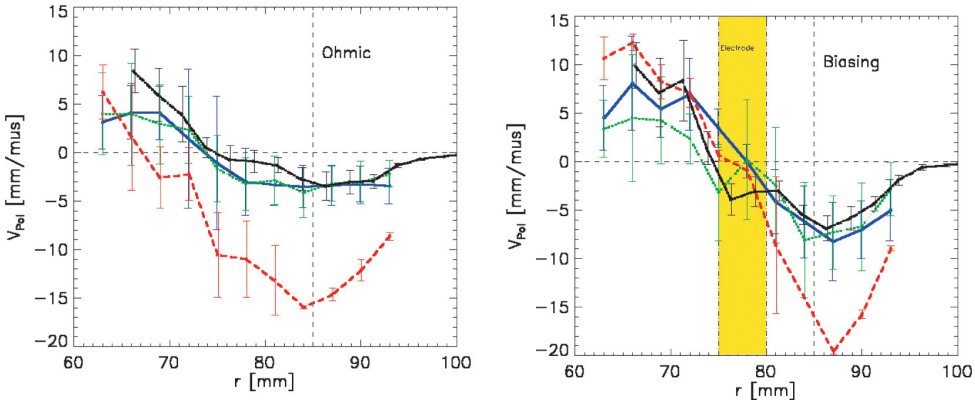

Figure 7. Radial profile of fluctuation velocities (blue and green lines), and flow velocity (red line) measured by the IGP. The black line is the $E \times B$ velocity deduced from the rake probe data. Left: Ohmic phase of the discharge. Right: biased phase of the discharge.

velocity and the fluctuation velocity follow each other very closely. In addition, the poloidal flow velocity is of the same order as the latter one within the separatrix ($r < 75$ mm). This indicates that turbulent structures are dragged by the poloidally rotating plasma. In contrast, there is a significant difference between the flow and $E \times B$ velocities observed within the SOL. The full explanation for this difference would require a better knowledge of the ion sound speed, which is needed to convert the Mach number, measured by the IGP to absolute units, $V = \sqrt{[(T_e + T_i)/M_i]}$. The electron and ion temperatures are assumed to be equal, $T_e = T_i$. However, our experiments indicate that the T_e, deduced from the IV characteristics of the Langmuir probe can be overestimated by a factor of 2–3. Taking this into account, the difference between the flow and $E \times B$ velocities becomes smaller [38]. Better agreement can be achieved, if the diamagnetic drift is taken into account, although in the case of CASTOR, the density and temperature profiles in the edge plasma are rather flat. The recent experimental data seem to confirm this conjectures.

Measurements of the parallel Mach numbers have also been performed at biasing [28]. In contrast to Alcator C-Mod results at L–H transition [40], we do not observe a dramatic increase of the toroidal rotation. This may be due to the much higher q values employed on CASTOR.

3.2.2. Full poloidal array. The experimental investigation of the full poloidal structure of electrostatic turbulence in the tokamak edge was performed using a poloidal probe array, similar to that already used in [41]. The diagnostic used for this work has been developed as part of a project aimed at attempting an active control of the edge turbulence, along the line of successful experiments performed on drift wave turbulence on linear machines [42]. In this paper only passive measurements are reported, both in standard Ohmic discharges and with edge biasing.

The turbulence control and diagnostic system consists of a poloidal ring of 32 plates surrounding the plasma column at the radius of 61 mm ([43] for details). Each plate is 7 cm long in the toroidal direction and 1 cm long in the poloidal direction and equipped with a flush mounted probe. All probes (plates) can measure the floating potential or the ion saturation current, allowing the estimation of the turbulent flux at this poloidal angle. The typical behaviour of the edge electrostatic turbulence as measured by the system described above is shown in figure 8.

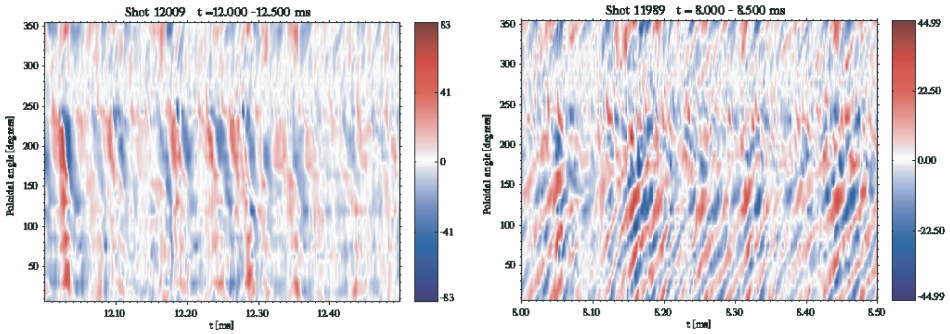

Figure 8. Spatial–temporal plot of potential fluctuations during Ohmic (left) and biasing (right) phase of a discharge.

This graph shows floating potential fluctuations as a function of time and poloidal angle. The amplitude of potential structures is marked by colours. It is possible to see a wave-like behaviour, with a dominant mode number, over most of the poloidal circumference. The wave amplitude is not constant, but undergoes oscillations with a typical period of 0.1 ms. It is important to notice that the observed pattern persists also on the high field side (around $\theta = 180^{\circ}$), so that the fluctuations do not show a ballooning character. Indeed, the main poloidal asymmetry is due to an attenuation of the fluctuations in the bottom region of the torus (around $\theta = 270^{\circ}$). This has been attributed to the fact that the CASTOR plasma is shifted downwards by 6–8 mm. The typical spatial–temporal plot of the floating potential fluctuations in unbiased plasmas displays time periodic structures propagating poloidally with $v_\theta \sim 3\,\mathrm{km\,s^{-1}}$. A poloidal Fourier analysis of the data shown in figure 8 has been performed and a dominant mode, namely the $m = 6$ mode, is found. In the experiments under study the q_a value was also around 6–7. This would imply that the edge safety factor at the edge determines the dominant poloidal wavenumber. In order to test this conjecture, some discharges with a ramping-down plasma current have been carried out. It has been confirmed that the poloidal mode number increases in time from 4.5 to 8, just proportionally to the q_a value.

At DC biasing produced by the biasing electrode located near the separatrix, the edge turbulence is modified by a sheared radial electric field, which is imposed to this region. The poloidal velocity of turbulent structures strongly increases and the poloidal mode number is reduced significantly down to $m = 1$–2.

3.2.3. Emissive probe results ([44] and references therein). In CASTOR a radially movable arrangement consisting of two emissive and two cylindrical (cold) probes has been used [45]. The probe head is inserted in such a way that the two emissive probes are on the same poloidal meridian, with a poloidal separation $d = 5.4$ mm between the probe tips. The cylindrical probes are located between the emissive probes, spaced toroidally by 5.6 mm, but displaced slightly to avoid mutual shadowing in the magnetic field. Usually one of the cold cylindrical probes was used to measure the ion saturation current and the other one was swept in order to record the *IV*-characteristics and to determine the average electron temperature.

The plasma potential and its fluctuations were measured by electron emissive probes in the edge plasma region of two fusion experiments: the ISTTOK (see later) and the CASTOR tokamaks. Into ISTTOK, three emissive probes were inserted outside the LCFS on different minor radii. In CASTOR, two poloidally separated emissive probes and two cold cylindrical probes, mounted on the same shaft, were used, which could be radially shifted outside and inside the LCFS. The advantage of a sufficiently emissive probe is that in principle the plasma

potential and its fluctuations can be measured directly, without being affected by electron temperature fluctuations or drifting electrons.

4. EB in regimes with ECR plasma heating in T-10

The H-mode was achieved by inserting the positively biased electrode into the plasma edge inside the limiter in the T-10 tokamak in regimes with electron–cyclotron resonant heating [46]. The H-mode is characterized by a decrease of D_α emission intensity, a rise of line-average plasma density and an increase of energy confinement time. The increase of core electron and ion temperatures during the EB implies the formation of the thermal barrier in addition to the barrier for particles.

4.1. Experimental set-up and plasma parameters

Experiments were performed on the T-10 tokamak having a major radius of $R = 1.5$ m. The minor plasma radius a_L determined by the rail limiter was 0.30 m (full poloidal limiter at 0.33 m).

The experiments were performed in deuterium. The average electron density n_e measured along a central chord was in the range 1×10^{19}–4×10^{19} m^{-3}, the toroidal magnetic field induction $B_t = 2.5$ T (this value corresponds to on-axis ECR heating), the plasma current $I_p = 200$–300 kA. The auxiliary electron–cyclotron heating power P_{aux} produced by gyrotrons (140 GHz) was varied from 200 to 800 kW. The ECRH power pulse length was 400 ms.

The electrode consists of a graphite head, 1.5 cm in radial direction, 5.5 cm in poloidal direction, and 4.5 cm in toroidal direction. It is inserted approximately 2 cm beyond the rail limiter into the plasma. The applied electrode voltage V_b is in the range -450–$+450$ V with respect to the wall (capacitor bank). Biasing experiments were performed in regimes with Ohmic heating and ECR heating. The ECRH power was below the threshold level for spontaneous L–H transition [47].

A radially movable triple probe (0.1 cm diameter and 0.3 cm long tungsten pins) is located at a toroidal angle of $\varphi = 90^\circ$ at the electron side of the rail limiter. This probe is used to measure ion saturation current, floating potential, electron temperature and their radial profiles on a shot-by-shot basis.

The radial electric field is deduced from a radial Langmuir probe array consisting of six carbon tips (length 2.5 mm, radius 2 mm). The tips measure the floating potential with a radial resolution of 3 mm. Since in these experiments the temperature gradient is substantially smaller than the gradient of the floating potential U_{fl}, we neglect the contribution of the temperature gradient. Therefore, the radial electric field is determined by the gradient of U_{fl} only.

The HIBP diagnostic was used to directly measure the local values of the plasma potential in the core and edge plasmas [48]. It is located at a toroidal angle of $\varphi = 180^\circ$ from the electrode. To obtain the radial potential profile the HIBP was used in the scanning mode. Scanning along the detector line allows to get a set of profiles in a single shot. The scanning was realized by periodical variation of the injection angle. The sampling frequency and bandwidth of the acquisition system allow the observation of slow oscillations.

4.2. Experimental results

At first it is necessary to note that in all regimes (with Ohmic and auxiliary ECR heating) no effect on the plasma parameters has been observed in a broad range of density and plasma current when a negative voltage was applied to the electrode. The H-mode has only been

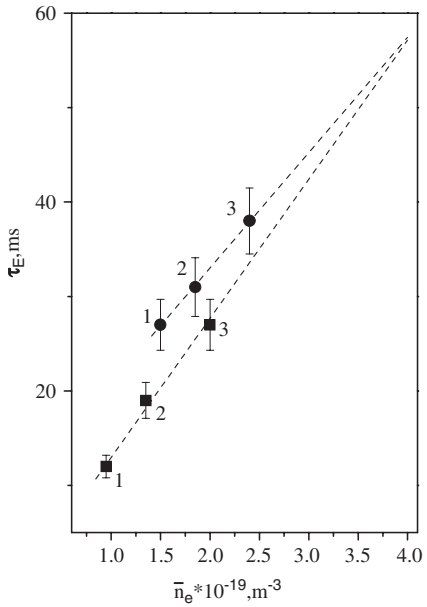

Figure 9. Dependence of the energy confinement time on the line-average electron density (■—before biasing, ●—during biasing). Points marked by the same number correspond to the same discharges.

achieved when a positive voltage with respect to the wall was applied to the electrode. The biased H-mode is characterized by the increase of the energy confinement time τ_E. Dependences of the energy confinement time on plasma density with and without EB are shown in figure 9. The τ_E growth during biasing is caused by the increase of the plasma density, the ion temperature as well as of the electron temperature. The ion and electron temperature growth is obviously related to the formation of a thermal barrier at the plasma edge of T-10.

Measurements of the electric field performed by using the probe array show that a strong positive radial electric field E_r is formed between the electrode and the rail limiter after voltage applying to the electrode (figure 10). E_r is sheared in this region and shows also negative values, which is important for turbulence suppression. This electric field has values up to 120 V cm^{-1}.

The region of the strong radial electric field formation coincides with a range of maximum density and electron temperature gradient increase. The appearance of the correlation reflectometry data points to the existence of a thin layer where the plasma turbulence displays perceptible changes. Such a layer lies between the electrode and the rail limiter and has a width of about 1 cm. No strong changes of the plasma turbulence were observed elsewhere in the plasma periphery.

EB in Ohmic regime is characterized by an insignificant growth of plasma density and small decrease of D_α emission intensity. A change of electron and ion temperature was not observed in Ohmic regime. A small increase of the energy confinement time is associated with a growth of the plasma density only.

The dependence of the plasma performance on vacuum chamber state was found in regime with positive biasing applying to the ECR heated plasma. No improvement of the energy confinement has been found if the wall was covered by deuterium containing graphite layers leading to enhanced seeding of deuterium and impurities to the plasma. Measurements in the plasma periphery in such a regime as well as in Ohmic regime were performed by HIBP [49].

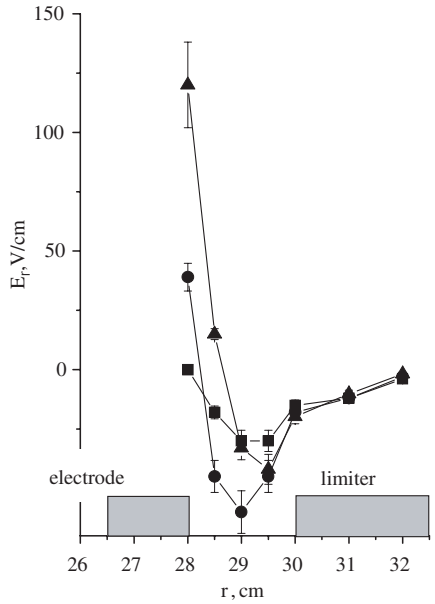

Figure 10. Radial profiles of the radial electric field (■—Ohmic mode; ●—ECRH, before biasing; ▲—ECRH, during biasing).

The evolution of the plasma potential and density profiles at positive EB $V_b = +400$ V with 5 ms scanning time and 20 ms intervals between scans has been studied. The radial profiles of the potential and density were simultaneously measured at the plasma edge, $0.8 < \rho < 1$ ($\rho = r/a_L$), both outside and inside the electrode radius $\rho_{el} \sim 0.9$. The extra plasma potential after biasing $\Delta\varphi(r, t) = \varphi(r, t) - \varphi(r, t_0)$ is shown in figure 11(*a*). It looks like a hill with a maximal value $\Delta\varphi_{peak}$, located in the vicinity of ρ_{el}. The initial potential profile $\varphi(r, t_0)$ is close to be flat. In the plasma interior, $0.8 < \rho < 0.85$, the extra potential is small. At both sides of the maximum of extra potential there are regions with strong electric field. The average values of these fields are close to each other, but their signs are opposite, $E_r \approx \pm 300$ V cm^{-1}. Thus we found that along with the strong field region previously observed by probes in other machines, in the electrode shadow, $\rho_{el} < \rho < 1$, another region with the strong field, located in the plasma interior, $0.85 < \rho < 0.9 = \rho_{el}$, may be formed. The evolution of the plasma density profile, obtained from the current of probing ions $\Delta I/I \sim \Delta n/n$, points out the appearance of two regions with increased density gradient, located close to the regions with strong electric field both inside and outside the potential peak. The time trace of the peak extra potential $\Delta\varphi_{peak}$ shows (see figure 11(*b*)) the fast rise up to the V_b value and the following slow evolution with a V_b decay timescale. It was found that the fluctuation energy of both the potential and the current of the probing ions in the frequency range under study (3–30 kHz) is suppressed in the whole radial observation area. This is a clear indication of the turbulent transport reduction due to edge plasma biasing. There were neither changes in the mean parameters nor in fluctuations in the case of the negative biasing.

5. Comparison of alternating EB and LB (ISTTOK)

In the ISTTOK tokamak EB and LB [50, 51] have been performed. LB has the advantage of using existing plasma facing components in the device contrary to EB where an object must

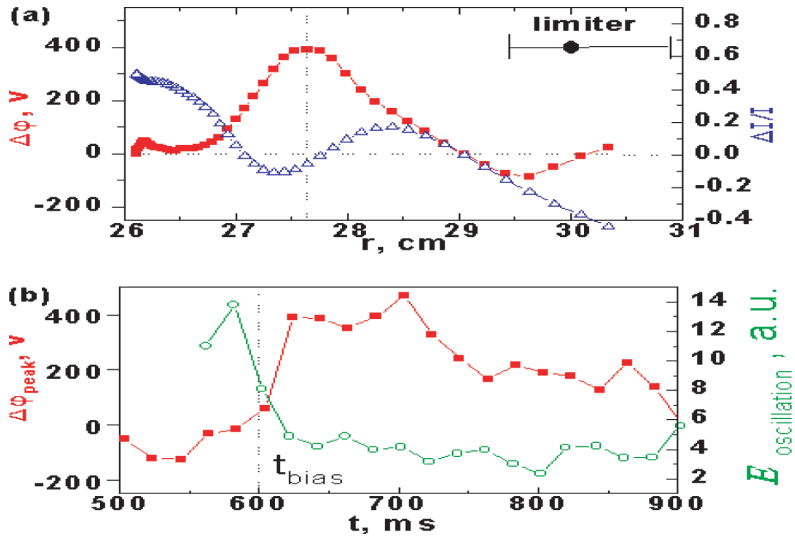

Figure 11. (*a*) Radial profiles of the extra plasma potential (■) and normalized changes of beam current (△). Uncertanty in the radial reconstruction are represented as an error bar in limiter position. (*b*) The time traces of the peak extra potential (■) and the energy of potential oscillations (○) in the frequency interval $3 < \nu < 30$ kHz.

be inserted into the plasma, which is not compatible with plasma operation in large devices. However, the modifications in E_r for LB are, in general, limited to the SOL.

5.1. Experimental set-up

ISTTOK is a large aspect ratio circular cross-section tokamak ($R = 46$ cm, $a = 8.5$ cm, $B_t \sim 0.6$ T, $\Delta\Phi = 0.22$ V s), which has two small localized limiters, one at the outer midplane and the other at the top. A poloidal limiter is used to determine the separatrix of the plasma ring. This limiter can also be biased to vary the space potential in the vicinity of the LCFS.

A typical ISTTOK discharge ($I_p \sim 4$–8 kA, $\tau_D \sim 30$–40 ms, $n_e(0) \sim 5$–10×10^{18} m^{-3}, $T_e(0) \sim 150$–250 eV, $\tau_E \sim 0.5$ ms, $\beta \sim 0.5\%$, $q(0) \sim 1$, $q(a) \sim 5$) has been taken as a reference.

Two different bias configurations have been studied on ISTTOK: LB and EB. Both DC (from -300 to $+300$ V) and alternating (50 Hz, 80–130 p V) bias voltages have been used; AC bias has the advantage of not only allowing the investigation of the effect of polarity in a single shot, but also determining biasing thresholds for confinement modifications. In the experiments reported here, the bias voltage is applied between the limiters/electrode and the vacuum vessel, and the electrode tip is situated at $r = 7$ cm (1.5 cm inside the limiter). A transformer is used to provide the alternating voltage and the phase is not synchronized with the discharge timer.

An array of Langmuir probes, toroidally located at about 180° from the limiter, has been used to study the influence of biasing on the boundary plasma. This array consists of two sets of three Langmuir probes, radially separated by 4 mm. Two tips of each set of triple probes, separated poloidally (3 mm), were used to measure the floating potential, V_f. The third tip was biased at a fixed voltage in the ion saturation current regime, I_{sat}. Measurements were taken at different radial positions in a series of similar and reproducible plasma shots.

The most recent measurements have been performed in ISTTOK with a radially movable arrangement of three emissive probes [45] (see also section 3), positioned in such a way

that the radial and the poloidal component of the electric field in the edge region can be recorded simultaneously. The radial, respectively poloidal spacing between the probes is 7 mm, respectively, 5.8 mm.

5.2. Experimental results

Although absolute comparison between LB and EB is not possible because experiments may have been performed under different machine conditions (e.g. wall conditioning), it is clear that the best confinement is achieved for positive EB. As expected, EB is more efficient than LB in modifying the radial electric field and confinement, LB mainly acting on the SOL; see, e.g. also TEXTOR LB results [52].

Both LB and EB can modify the plasma behaviour, however, EB introduces larger alterations in the plasma parameters. The stronger modification in plasma potential V_{p} observed for EB results in larger electric fields and consequently larger alterations in confinement. For the same applied voltage ($\Delta V_{\mathrm{bias}} = 240\,\mathrm{V}$), the modification in V_{p} imposed by EB ($\Delta V_{\mathrm{p}} = 80\,\mathrm{V}$) is much larger than that for LB ($\Delta V_{\mathrm{p}} = 30\,\mathrm{V}$).

A good correlation between confinement modifications and $E_r \times B$ shear has been found for positive EB suggesting that confinement enhancement originates at the edge plasma as a consequence of the formation of a particle transport barrier just inside the limiter. In these bias experiments a radial electric field has been imposed in a controlled fashion and the issue of causality between E_r and confinement has been investigated in detail.

With LB the behaviour of the cross-field particle flux ($\Gamma_{E\times B} = \langle \tilde{n}\tilde{E}_\theta \rangle / B$), during biasing, is similar to that of I_{sat}. Particle losses in the main plasma increase for positive applied voltages and decrease for negative ones.

With EB spectral analysis of both I_{sat} and $\Gamma_{E\times B}$, in the main plasma shows a large decrease of the turbulence level for positive bias, in particular for frequencies between 20 and 50 kHz, when compared with results obtained for negative bias.

6. EB in a reversed field pinch experiment (RFX)

The potential for L–H transitions in reversed field pinch (RFP) configurations is a promising area of investigation since it has been noted that the edge physics of these configurations manifests many similarities with that of the tokamaks and stellarators [53]. Among these similarities it is worth mentioning that most of the particle transport at the edge is driven by electrostatic turbulence and that a spontaneous sheared $E \times B$ flow occurs in the edge region. Sheared flow in a RFP plasma was observed in RFX [54], in EXTRAP-T2 [55] and in MST [56]. In RFX the spontaneous flow shear was suggested to influence the particle diffusion coefficient profile at the edge [57] since the shearing frequency associated with electrostatic turbulence was found to be close to that required by the turbulence decorrelation criterion [58]. The spontaneous or externally driven transition to regimes of improved confinement observed in RFPs was associated with a modification of this shear at the edge [53, 56, 58] .

For the first time in a reversed field pinch experiment, the evidence of a causality between an externally driven modification of the $E \times B$ velocity shear at the edge and a reduction of the electrostatic particle flux has been established [59].

6.1. Experimental set-up

RFX is a toroidal device with minor radius $a = 0.457\,\mathrm{m}$ and major radius $R = 2\,\mathrm{m}$ which confines plasmas in RFP configuration. Two electrodes have been inserted into the plasma. Most of the data refer to an insertion at $r/a = 0.81$.

The electrodes can be positively or negatively biased with respect to the vacuum vessel. The results presented here pertain to negative biasing which increases the $E \times B$ flow present at the edge in standard conditions. It is worth noting that in the RFP the magnetic field in the edge region is mainly poloidal, so that the $E \times B$ drift is mainly directed in the toroidal direction. This drift is much larger than the diamagnetic one.

The radial electric field has been derived by a set of probes aligned in the radial direction and simultaneously measuring the floating potential in seven positions equally spaced by 8 mm. This probe, called 'rake probe', was placed at $\varphi = 217^{\circ}$.

Another probe, named fluctuation insertable probe (FLIP), has been used to measure the electrostatic fluctuations. In this experimental campaign a 5-pin balanced triple Langmuir probe and a pin measuring the floating potential were used. The two measurements were aligned in the toroidal (i.e. cross-field) direction, at a distance of 44 mm. The FLIP was located at $\varphi = 247^{\circ}$ and it has been moved on a shot-by-shot basis to scan the plasma up to $r/a = 0.94$, which is the region where the electrostatic particle flux is highest [57].

The experiment has been operated with hydrogen plasma at low plasma current ($I_{\mathrm{p}} < 350\,\mathrm{kA}$) in order to minimize the plasma interaction with the electrodes and the probes.

6.2. Experimental results

During biasing the $E \times B$ shear increases by a factor of 2 for $r/a > 0.92$. The profiles come back to the original shape after the biasing, showing that the change was indeed induced by the electrode and was not a result of a spontaneous evolution of the plasma [59].

During the same edge biasing operation a strong reduction of the particle flux driven by electrostatic turbulence has been observed. The flux reduction results from combined reductions of transverse wavenumber, coherence and phase, whereas the potential fluctuation level reduction is small, and the density fluctuation level shows an increase. This latter increase can be explained because of a local increase of the average density, so that the normalized fluctuation level actually remains almost constant.

In order to better evaluate how structures of different size arising in the turbulence contribute to the total flux, we have plotted in figure 12 the quantities as a function of the transverse wavenumber. In standard conditions the particle flux turns out to be driven by transverse wavenumbers up to $50\,\mathrm{m}^{-1}$, i.e. by structures with a transverse characteristic length larger than 10 cm. The product of the typical wavenumber and the ion Larmor radius is of the order of 0.1, similar to what is found in tokamaks. The effect of doubling the velocity shear by edge biasing is to approximately halve the maximum wavenumber relevant for transport, $k_{\perp\,\mathrm{max}}$, reducing it to $25\,\mathrm{m}^{-1}$. The other plots of figure 12 show that the coherence at a given wavenumber is less affected, whereas the flux reduction is due to both a reduction in the ϕ fluctuation level and a change in the relative phase between potential and density. The $\sin\alpha_{n\phi}$ behaviour is what determines the particle flux profile, and the change in phase appears to be the most important effect, at least for wavenumbers larger than $20\,\mathrm{m}^{-1}$. The halving of $k_{\perp\,\mathrm{max}}$ induced by the biasing could be understood in terms of the Biglari–Diamond–Terry (BDT) criterion for the effect of the velocity shear on turbulence [58].

The energy flux driven by electrostatic turbulence, which in the RFX edge was found to be mainly convective and of the order of 30% of the total transport losses, has been also measured during the edge biasing. It turns out that it remains mainly convective, and therefore drops by the same factor as the particle flux.

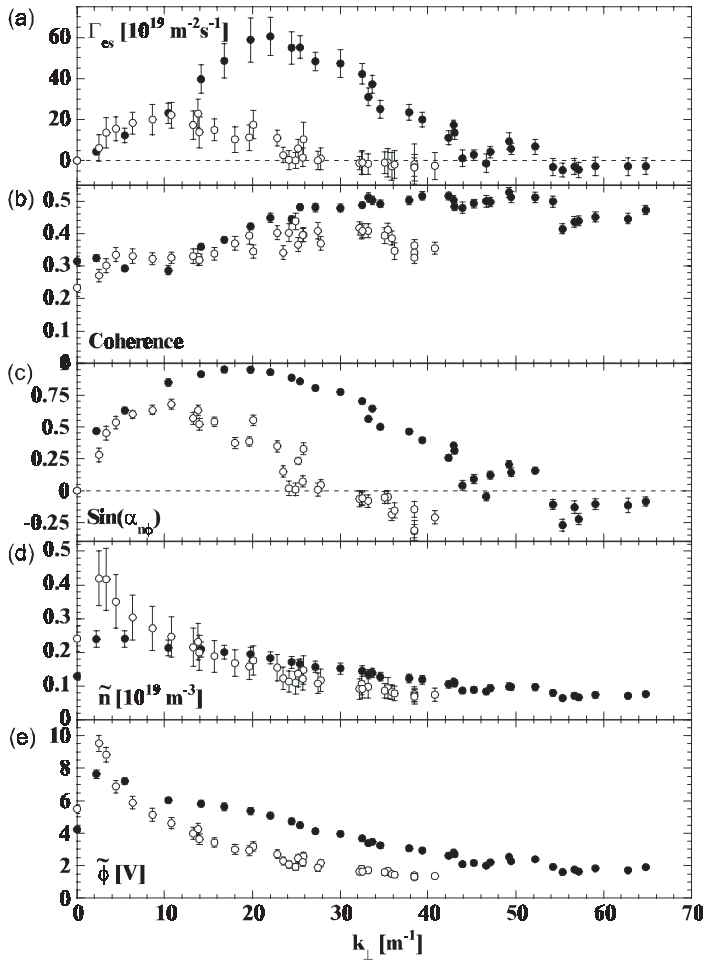

Figure 12. Frequency-resolved values of particle flux (*a*), n–ϕ coherence (*b*), sine of the n–ϕ cross-phase (*c*), density fluctuation level (*d*) and plasma potential fluctuation level (*e*) in normal conditions (●) and during the electrode action (○) are plotted as a function of the transverse (toroidal) wavenumber. The data were collected at $r/a = 0.97$ and are averaged over 26 discharges. Error bars show the standard error.

7. Summary and outlook

New and complementary detailed experimental evidence of the correlation between sheared $E \times B$ flow and the establishment of edge transport barriers and improved confinement has been obtained in the circular limiter tokamaks TEXTOR, CASTOR, T-10 and ISTTOK, as well as in the reversed field pinch RFX where a radial electric field (E_r) and resulting $E \times B$ shearing are externally applied to the plasma in a controlled way using a biased electrode.

The biasing experiments on TEXTOR with the well diagnosed plasma edge using probes to measure all relevant quantities such as electric field, parallel and perpendicular plasma flow, fluctuation and turbulent particle flux, have given the first proof for transport suppression due to sheared $E \times B$ flows. Quantitative analysis has shown that the diffusion coefficient decreases at the shearing rate predicted by theory. These findings are in good agreement with measurements

of the fluctuating quantities, which contribute to the turbulent transport. Changes in the cross-phase are essential for substantial quenching of turbulence. A one-dimensional fluid model, in which parallel viscosity and neutral friction were already identified as important components to explain the very important and localized electric fields has been developed. Recent work has focused on the convection and shear viscosity, introduced by anomalous radial flows, and their subsequent reduction by the quenching of the turbulence. It has been shown that without the quenching of the turbulence, it is impossible to explain the magnitude and the shape of the measured electric field. The destruction of parallel viscosity by strong poloidal plasma rotation has been identified to cause a bifurcation in the electric field. Rapid changes in the polarization driving current have been used as a diagnostic tool to study the causality between rotational shear and confinement improvement. The flow shear is clearly leading the transport changes and as a result, a hysteresis between the imposed shearing rate and the particle diffusion coefficient arises.

The scaling of plasma turbulence suppression with velocity shear has been established, revealing the cross-phase as a key element. Two important results should be noted: first that the scaling of the cross-phase term is as strong as that of the turbulence amplitudes, revealing the cross-phase as a key element in the suppression of turbulent transport. Second that there is a difference in the scaling of the cross-phase between the positive and negative shear regions, an effect not included in the theories, which are phase-sign blind and therefore these results should be considered closely by theoreticians. First measurements of the suppression of electron temperature fluctuations in a strongly sheared velocity field have been made. Reduction in poloidal electric field, temperature, and density fluctuations across the shear layer lead to a reduction of the anomalous conducted and convected heat fluxes resulting in an energy transport barrier that is measured directly.

The probe diagnostics on TEXTOR will be enhanced to allow electric field and plasma flow measurements with a higher spatial and temporal resolution and to determine the Reynolds stress. The parameter study of the effect of $E \times B$ shear on turbulent transport will be completed. Further experimental schemes are under development to contribute to SOL engineering of later future fusion tokamaks.

The biasing arrangement and the plasma flow and turbulence measurements on CASTOR offered a first experimental proof of the theoretical prediction that imposing a boundary condition by (non-intrusive) separatrix biasing is an efficient way to create strongly sheared electric fields, thereby affecting plasma flows and decorrelating turbulent structures, and creating an edge transport barrier in the proximity of the separatrix, which leads to improved confinement. It appears as if the conventional scenario of triggering the L–H transition by means of the power exceeding a given threshold, is a 'brute force' solution. More subtle methods like separatrix biasing or e.g. also peripheral pellet injection [29] appear to be operative.

The impact of sheared $E \times B$ flow on edge turbulent structures has been measured directly using an optimized Gundestrup probe, a comprehensive set of electrostatic probe arrays as well as emissive probes which provide direct plasma potential fluctuation measurements. The Gundestrup probe provides the simultaneous measurement of toroidal and poloidal flows, and of electrostatic turbulence, and has demonstrated the correlation between sheared $E \times B$ flow and reduction of turbulence. Very recently, a novel concept has been suggested to measure the electron temperature fluctuations and a prototype of the so-called tunnel probe has been successfully tested on CASTOR. Measurements with a full poloidal array with 32 electrodes plus Langmuir probes have revealed quasi-coherent electrostatic waves in the SOL with a dominant poloidal mode number (6) equal to the edge safety factor. At DC biasing with an electrode located near the separatrix, the edge turbulence is modified by a sheared radial electric

field, which is imposed to this region. The poloidal velocity of turbulent structures strongly increases and the poloidal mode number is reduced significantly down to 1–2.

The first experimental campaign on CASTOR dedicated to the turbulence control shows that standing and propagating waves in the frequency range of 10–40 kHz and the mode number range $m_\theta = 2$–8 can be successfully excited in the SOL using the poloidal ring of electrodes. The possibility to modify the turbulent flux in the SOL both with constant and modulated biasing is demonstrated. In both cases, a reduction of the local flux is achieved. However the constant and modulated biasing produce different effects on the flux structure and its bursty behaviour. The static field suppresses the large amplitude bursts propagating outwards while the oscillating field produces inward bursts of the flux without suppressing outward bursts. The turbulent flux is reduced due to a strong de-phasing between density and poloidal electric field fluctuations in the case of modulated biasing.

However, some uncertainties remain in the determination of the flux because of the probe separation and the absence of global particle flux measurements. More detailed analysis of the SOL plasma will be the subject of future experiments.

In spite of some demurs concerning the accuracy of the floating potential of strongly emissive probes in terms of indicating the true value of the plasma potential, we believe that the method to determine the plasma potential by an electron-emissive probe is able to deliver at least a better approximation for the plasma potential than the floating potential of a cold probe. Moreover, in any case the floating potential of an emissive probe shows a weaker dependence on drifting electrons and electron temperature fluctuations than a cold probe.

The first biasing experiments performed on the T-10 tokamak have shown that positive voltage applied to an electrode results in an increase of core electron and ion temperatures and of energy confinement time in regimes with ECR auxiliary heating, in contrast to the Ohmic regime. Hence, edge biasing is clearly improving the global performance of ECR heated discharges. Reflectometry shows the existence of a narrow plasma layer where strong changes of turbulence levels occur. A HIBP diagnostic has been used to directly measure the local values of the plasma potential in the vicinity of the electrode radius, outside as well as inside, showing two regions with strong radial electric field and a strong reduction of plasma potential and density fluctuations in the vicinity of the electrode radius, outside as well as inside. To explain the different plasma behaviour in OH and ECRH regimes it is planned to carry out the measurements of profiles of radial electric field, toroidal and poloidal plasma rotation velocity in the plasma periphery between the electrode and limiter.

On the ISTTOK tokamak the influence of alternating positive and negative EB and LB is studied. EB is found to be more efficient in modifying E_r and confinement. The best confinement improvement is obtained with positive EB, showing a good correlation between confinement changes and $E \times B$ shear. Negative (positive) LB leads to improved (deteriorated) confinement and better (worse) stability of the plasma column. Coordinated emissive probe direct measurements of the plasma potential and its fluctuations are planned on ISTTOK and CASTOR.

The $E \times B$ velocity and its shear have been modified in the edge of the RFX reversed field pinch experiment by a biasing experiment performed with electrodes inserted into the plasma. Causality between an increase in the $E \times B$ velocity shear and a decrease of the particle flux driven by electrostatic turbulence has been observed. The decrease of the particle flux has been found to be mainly due to a change of the relative phase between density and plasma potential fluctuations. The results confirm the role of sheared flow in transport suppression in reversed field pinches and show remarkable similarities with those found in other magnetic configurations.

Acknowledgments

This work was supported by the INTAS Grant No 2001-2056. That of the Kurchatov team was also supported by Russian Basic Research Foundation, Grant Nos 02-02-17727, 02-02-06609 and 00-15-96536. The work of the IPP Prague team was partially supported by the Grant Agency of the Czech Republic, Grant No 202/03/0786.

References

[1] Ida K 1998 *Plasma Phys. Control. Fusion* **40** 1429
[2] Taylor R J *et al* 1989 *Phys. Rev. Lett.* **63** 2365
[3] Weynants R R and Van Oost G 1993 *Plasma Phys. Control. Fusion* **35** B177
[4] Weynants R R 2001 *J. Plasma Fusion Res. Ser.* **4**
[5] Van Oost G *et al* 2001 *Czech. J. Phys*. **51** 957
[6] Wagner F *et al* 1982 *Phys. Rev. Lett.* **49** 1408
[7] Groebner R J *et al* 1990 *Phys. Rev. Lett.* **64** 3015
[8] Ida K *et al* 1990 *Phys. Rev. Lett.* **65** 1364
[9] Biglari H, Diamond P H and Terry P W 1990 *Phys. Fluids* B **2** 1
[10] Ritz C P *et al* 1990 *Phys. Rev. Lett.* **65** 2563
[11] Ware A S, Terry P W, Carreras B A and Diamond P H 1998 *Phys. Plasmas* **5** 173
[12] Rozhansky V, Tendler and Voskoboinikov M S 1996 *Plasma Phys. Control. Fusion* **38** 1327
[13] Weynants R R *et al* 1992 *Nucl. Fusion* **32** 837
[14] Jachmich S *et al* 1998 *Plasma Phys. Control. Fusion* **40** 1105
Cornelis J *et al* 1994 *Nucl. Fusion* **34** 171
[15] Jachmich S, Van Oost G, Weynants R R and Boedo J A *Czech. J. Phys.* **48** 32
[16] Van Goubergen H *et al* 1999 *Plasma Phys. Control. Fusion* **41** L17
[17] Boedo J A *et al* 1999 *Rev. Sci. Inst.* **70** 2997
[18] Jachmich S, Van Schoor M and Weynants R R 2002 *Proc. 29th EPS Conf. on Plasma Physics and Control. Fusion (Montreux, 2002)* vol 26B (ECA) O-1.01, to be published
[19] Weynants R R, Jachmich S and Van Oost G 1998 *Plasma Phys. Control. Fusion* **40** 635
[20] Jachmich S and Weynants R R 1999 *Czech. J. Phys.* **49** 191
[21] Jachmich S *et al* 2000 *Plasma Phys. Control. Fusion* **42** A147
[22] Staebler G *et al* 1994 *Phys. Plasmas* **1** 909
[23] Shaing K C *et al* 1990 *Phys. Fluids* B **2** 1492
[24] Zhang Y Z and Mahajan S M 1992 *Phys. Fluids* B **4** 1385
[25] Boedo J A *et al* 2000 *Nucl. Fusion* **40** 1397
[26] Boedo J A *et al* 2002 *Nucl. Fusion* **42** 117
[27] Boedo J A *et al* 2000 *Phys. Rev. Lett.* **84** 2630
[28] Van Oost G, Stöckel J, Hron M, Devynck P, Dyabilin K, Gunn J P, Horacek J, Martines E and Tendler M 2001 *J. Plasma Fusion Res. Ser.* **4** 29–35
[29] Tendler M, Van Oost G and Stöckel J 2002 *Comments Modern Phys.* **2** C203
[30] Petrzilka J and Stöckel J 1998 *Contrib. Plasma Phys.* **38** 74–9
[31] Blauel J, Endler M, Niedermayer H, Schubert M and Thomsen H 2002 *New J. Phys.* **4** 38.1–38.38
[32] Stöckel J *et al* 1999 *Plasma Phys. Control. Fusion* A **41** A577–85
[33] Martines E, Hron M and Stöckel J 2002 *Plasma Phys. Control. Fusion* **44** 351–9
[34] Martines E *et al* 2002 *Czech J. Phys.* D **52** D13–24
[35] Gunn J P *et al* 2001 *Phys. Plasmas* **8** 1995
[36] Dyabilin K, Hron M, Stöckel J and Zacek F 2002 *Contrib. Plasma Phys.* 99
[37] Gunn J P 2001 *Phys. Plasmas* **8** 1040
[38] Gunn J P *et al* 2002 *Czech. J. Phys.* **52** 1107
Gunn J P *et al* 2002 *Proc. 19th IAEA Fusion Energy Conf. (Lyon, 2002)* (paper EX/P1-06) to be published
[39] Gunn J P *et al* 2001 *Czech. J. Phys.* **51** 1001–10
[40] Rice J E *et al* 2001 *Phys. Plasmas* **7** 1825
[41] Tynan G R *et al* 1992 *Phys. Rev. Lett.* **68** 3032
[42] Schröder C *et al* 2001 *Phys. Rev. Lett.* **86** 5711
[43] Hron M *et al* 2002 *Proc. 29th EPS Conf. on Plasma Phys. Control. Fusion (Montreux, 2002)* vol 26B (ECA) P-5.043

[44] Schrittwieser R *et al* 2002 *Plasma Phys. Control. Fusion* **44** 567
[45] Balan P *et al* 2003 *Rev. Sci. Inst.* **74** in press
[46] Kirnev G S *et al* 2001 *Czech. J. Phys*. **51** 1011
[47] Kislov D A *et al* 2001 *Nucl. Fusion* **41** 1473
[48] Melnikov A *et al* 2000 *J. Plasma Fusion Res. Ser.* **3** 917
[49] Melnikov A, Eliseev L, Perfilov S, Mavrin V, Lysenko S, Razumova K, Dnestrovskij Yu and Krupnik L 2002 *Proc. 29th EPS Conf. on Plasma Phys. Control. Fusion (Montreux, 2002)* vol 26B (ECA) P-1.115
[50] Cabral J A C *et al* 1998 *Plasma Phys. Control. Fusion* **40** 1011
[51] Cabral J A C *et al* 2002 *Proc. 28th EPS Conf. on Plasma Phys. Control. Fusion (Funchal, 2002)* vol 25A (ECA) p 605
[52] Doerner R P *et al* 1994 *Nucl. Fusion* **34** 975
[53] Antoni V 1997 *Plasma Phys. Control. Fusion* **39** B223
[54] Antoni V *et al* 1997 *Phys. Rev. Lett*. **79** 4814
[55] Möller A 1997 *Proc. 24th EPS Conf. on Controlled Fusion and Plasma Physics (Berchtesgaden, 1997)* (EPS, Geneva) part III, p 1273
[56] Chapman E *et al* 1998 *Phys. Rev. Lett.* **80** 2137
[57] Antoni V *et al* 1998 *Phys. Rev. Lett.* **80** 4185
[58] Craig D *et al* 1997 *Phys. Rev. Lett.* **79** 1865
[59] Antoni V *et al* 2000 *Plasma Phys. Control. Fusion* **42** 83

Summary of Comments on p152168

Page: 1

Sequence number: 1
Author:
Date: 2/4/03 6:08:00 PM
Type: Note
Pub: Please check the article type

Page: 22

Sequence number: 1
Author:
Date: 2/4/03 6:09:16 PM
Type: Note
Author: Please supply initials for Tendler in ref 12

Sequence number: 2
Author:
Date: 2/4/03 6:09:37 PM
Type: Note
Author: Please provide year for ref 15

Sequence number: 3
Author:
Date: 2/4/03 6:09:47 PM
Type: Note
Author: Please update ref 18, 38, 45